

Solidification kinetics of a Cu-Zr alloy: ground-based and microgravity experiments

This content has been downloaded from IOPscience. Please scroll down to see the full text.

2017 IOP Conf. Ser.: Mater. Sci. Eng. 192 012028

(<http://iopscience.iop.org/1757-899X/192/1/012028>)

View [the table of contents for this issue](#), or go to the [journal homepage](#) for more

Download details:

IP Address: 141.35.54.187

This content was downloaded on 19/04/2017 at 17:44

Please note that [terms and conditions apply](#).

Solidification kinetics of a Cu-Zr alloy: ground-based and microgravity experiments

P K Galenko^{1,2}, R Hanke¹, P Paul¹, S Koch¹, M Rettenmayr¹, J Gegner³, D M Herlach^{3,4}, W Dreier⁵ and E V Kharanzhevski⁵

¹ Friedrich-Schiller-Universität Jena, Otto-Schott-Institut für Materialforschung, D-07743 Jena, Germany

² Ural Federal University, Laboratory of Multi-Scale Mathematical Modeling, 620002 Ekaterinburg, Russia

³ Deutsches Zentrum für Luft- und Raumfahrt, Institut für Materialphysik im Weltraum, 51170 Köln, Germany

⁴ Ruhr-Universität, Physikalisch-Astronomische Fakultät, 44810 Bochum, Germany

⁵ Udmurt State University, Faculty of Physics and Energetics, 426037 Izhevsk, Russia

E-mail: peter.galenko@uni-jena.de

Abstract. Experimental and theoretical results obtained in the MULTIPHAS-project (ESA-European Space Agency and DLR-German Aerospace Center) are critically discussed regarding solidification kinetics of congruently melting and glass forming Cu₅₀Zr₅₀ alloy samples. The samples are investigated during solidification using a containerless technique in the Electromagnetic Levitation Facility [1]. Applying elaborated methodologies for ground-based and microgravity experimental investigations [2], the kinetics of primary dendritic solidification is quantitatively evaluated. Electromagnetic Levitator in microgravity (parabolic flights and on board of the International Space Station) and Electrostatic Levitator on Ground are employed. The solidification kinetics is determined using a high-speed camera and applying two evaluation methods: “Frame by Frame” (FFM) and “First Frame – Last Frame” (FLM). In the theoretical interpretation of the solidification experiments, special attention is given to the behavior of the cluster structure in Cu₅₀Zr₅₀ samples with the increase of undercooling. Experimental results on solidification kinetics are interpreted using a theoretical model of diffusion controlled dendrite growth.

1. Introduction

A valuable progress in the investigation of glass forming metals and alloys has been made since their discovery by Turnbull [3]. The development of containerless processing techniques, especially using different methods of levitation, provided a new ability to reach deep undercoolings and to investigate solidification into the crystalline or glassy state [1]. A favourable advantage of the containerless methods is the prevention of heterogeneous nucleation, which in turn allows for a better investigation of the effects of high undercoolings and rapid growth conditions on the solidification of metals and alloys.

The present work is devoted to a systematic view on recent results obtained regarding solidification of the congruently melting and glass forming Cu₅₀Zr₅₀ alloy. Wang et al. [4] showed that CuZr exhibits a maximum growth velocity at an undercooling of ~200 K and a steep decline at higher undercoolings, with the according deviation from the Arrhenius law in the dynamic viscosity where the structure of the



liquid changes, as pointed out by Kelton et al. [5]. Furthermore, Kobold [6] finds an additional growth path with lower velocities than the ones found by Wang et al., with the question arising where this comes from. Motivation for the present research is that a theoretical model provided by H. Wang et al. [7] for solidification kinetics does not sufficiently explain all experimental data points obtained by Q. Wang et al. [4] and thus the need for a more accurate model arises. In order to study the peculiarities of $\text{Cu}_{50}\text{Zr}_{50}$, ground-based and microgravity experiments have recently been carried out in parabolic flights.

2. Experimental methods

Electrostatic and electromagnetic levitation techniques, where the heterogeneous nucleation may effectively be prevented (at least from the outer surface of the sample), are employed to investigate the kinetics of dendritic solidification under the conditions of normal gravitational forces (1g) and microgravity (μg).

Electromagnetic levitation [8] is used in terrestrial laboratories at DLR Köln and Jena University (see Figure 1). The temperature is measured contactless by a two-colour pyrometer with an accuracy of ± 5 K. An alternating electromagnetic field is causing both a levitation force and heating of the sample due to eddy currents. No extra heating source is required. Levitation and heating cannot be controlled separately. Therefore, a helium gas stream is needed to transfer the heat from the sample to the environment.

The limitation of coupled heating and levitating is overcome if electromagnetic levitation is applied in microgravity. Using the concept of two independently working coil systems, a quadrupole field for positioning, and a dipole field for heating, positioning and heating can be controlled separately at an increase of the efficiency from 1 to 30 % [9]. An Electromagnetic Levitator (EML) is in use on board the International Space Station.

To measure the dendrite growth velocity, a high-speed camera is used that records the advancement of the intersection line of the solidification front with the sample surface with 500 frames/sec [10].

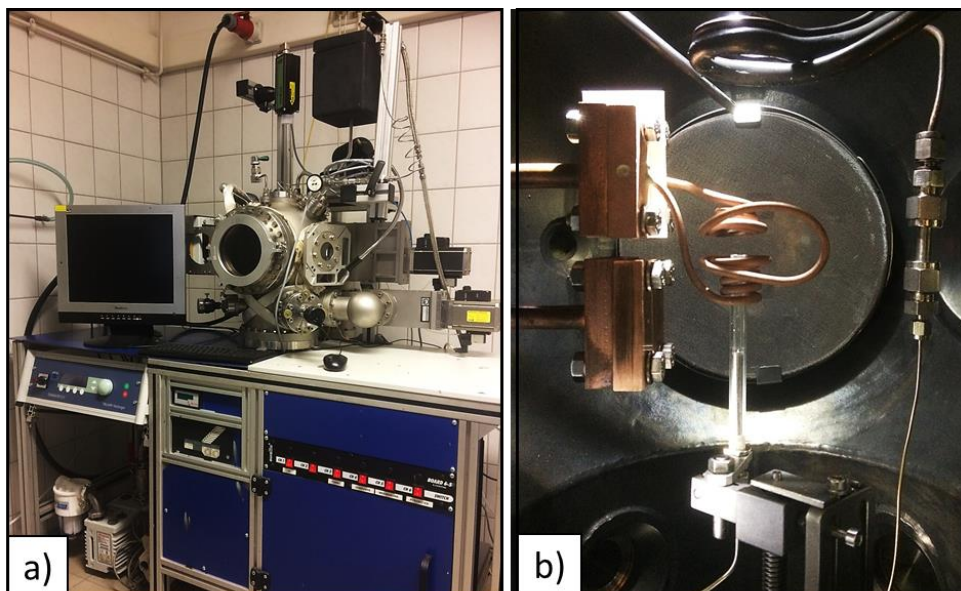


Figure 1. Experimental setup of electromagnetic levitation facility at Otto Schott Institute of Materials Research at Friedrich Schiller University Jena. (a) A general view of EML device. (b) Sample holder with a cooling system and an alternating current coil.

3. Methods of evaluation of solidification kinetics

The experimental solidification velocity for an initial undercooling is evaluated by recalescence fronts. Under fronts of recalescence we understand an envelope of growing dendrite tips, nucleation points or corners of crystalline patterns having specific crystallographic orientation. Figure 2 shows snapshots of a propagating recalescence front, defined by an envelope of the dendrite growth area.

Two different methods for evaluation of crystal growth kinetics are used. These are: evaluation with the Frame-by-Frame Method (FFM) and the First Frame-Last Frame Method (FLM). The FLM measures the growth velocity as a function of droplet radius R and the time interval Δt_{tot} from the beginning of dendrite growth until its end:

$$v_{\text{FLM}} = \frac{2R}{\Delta t_{\text{tot}}} . \quad (1)$$

Proper measurement is achieved by setting up the camera and a mirror to record images of a large part of the surface area of the sample. Details can be further examined by mapping these images onto a 3d spherical model [6]. Therefore, the FFM is used for the estimation of growth velocity as a function of the evolving growth area Δr (estimated as a spherical area) during the interval between two frames Δt_{fr} :

$$v_{\text{FFM}} = \frac{\Delta r}{\Delta t_{\text{fr}}} . \quad (2)$$

One can obviously suppose that the calculated growth velocities using FLM and FFM should be (almost) the same if only one nucleation center is observed (as shown in Fig. 2). Four videos with recalescence occurring at various undercoolings were analyzed. As shown in Table 1, indeed, measurements with just one recalescence (nucleation) center give approximately the same growth velocity measured by these two methods. In contrast, three recalescence centers yield a large difference in the measured velocities.

Table 1. Data of microgravity investigations: measured dendrite growth velocities (evaluated by FLM and FFM) in undercooled $\text{Cu}_{50}\text{Zr}_{50}$ alloy samples processed in the Electromagnetic Levitator during parabolic flights.

No. experiment	Undercooling (K)	Recalescence centers (nuclei points)	Velocity by FLM (mm/s)	Velocity by FFM (mm/s)
00	95	1	8,61	9,77
01	170	1	13,61	11,50
04	145	1	21,85	17,68
05	195	3	31,71	11,69

4. Results

Data sets for dendrite growth velocities in CuZr samples have been obtained under microgravity conditions in parabolic flights (Airbus A310 Zero-G). During these flights, the airplane is accelerating periodically until it reaches an angle of 47 degrees, then stopping acceleration and starting the descent and microgravity phase for about 20 seconds. This flight pattern results in parabolae - hence the name - with microgravity phases persisting for each parabola between the reversal points of the flight curve. As a result, during every 20-22 seconds, measurements of dendrite growth velocity are obtained.

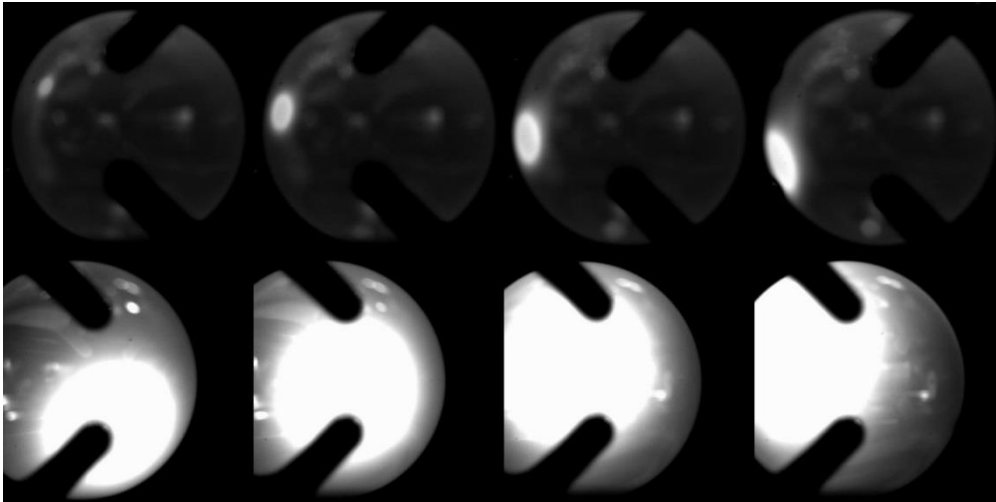


Figure 2. Different stages of solidification front evolving from one nucleation center (bright spot on top left) at an undercooling of 145 K. Top left: a few milliseconds after the start of growth. Top right: after 7 ms. Bottom left: after 76 ms. Bottom right: after 84 ms.

The growth velocities obtained via FLM and FFM are compared with previous studies in Fig. 3. Wang et al. [4] and Kobold [6] find a maximum in velocity for $\text{Cu}_{50}\text{Zr}_{50}$ at undercoolings in the region of 200 K as well as a steep decline of velocities at undercoolings above 250 K. Furthermore, Kobold [6] obtained a second growth regime (see blue squares for the low velocity sequence of data in Fig. 3) which is also confirmed by our present measurements (see three points obtained by both FLM and FFM in the region of undercooling 170-195K). Therefore, to explain this second behavior, the model of the diffusion-limited growth should be extended for prediction of metastable phase formation taking into account the process of phase selection.

For the undercooling of 95 K, FLM and FFM agree with other data points. This also applies to FFM at 145 K, although the FLM value appears to be somewhat too high. At 170 K, both values reside near the lower growth regime. At the undercooling of 195 K there is a strong deviation between FLM and FFM. The FLM value is nearly three times as high as the FFM value. Evaluation of the corresponding video shows three recalescence centers that lead to assuming too fast solidification if FLM is utilized. However, using the FFM, the recently measured velocity is close to the lower data points (see blue squares in Fig. 3).

Experimental data on growth kinetics represent a special interest for our theoretical advancement in solidification kinetics. Using a dendrite growth model based on the diffusion-limited approach to glass forming alloys, Wang et al. [7] provided a comparison of their calculation with experimental data. Figure 3 shows this comparison (see the solid line as predicted by Wang et al.). It can be seen that the modeling results describe the experimental data quite well up to the maximum velocity around the undercooling of 210-220 K. The velocity maximum in Fig. 3 is consistent with the point where gradual freezing of atoms and the decrease of their mobility starts such that the transition to sluggish growth kinetics occurs.

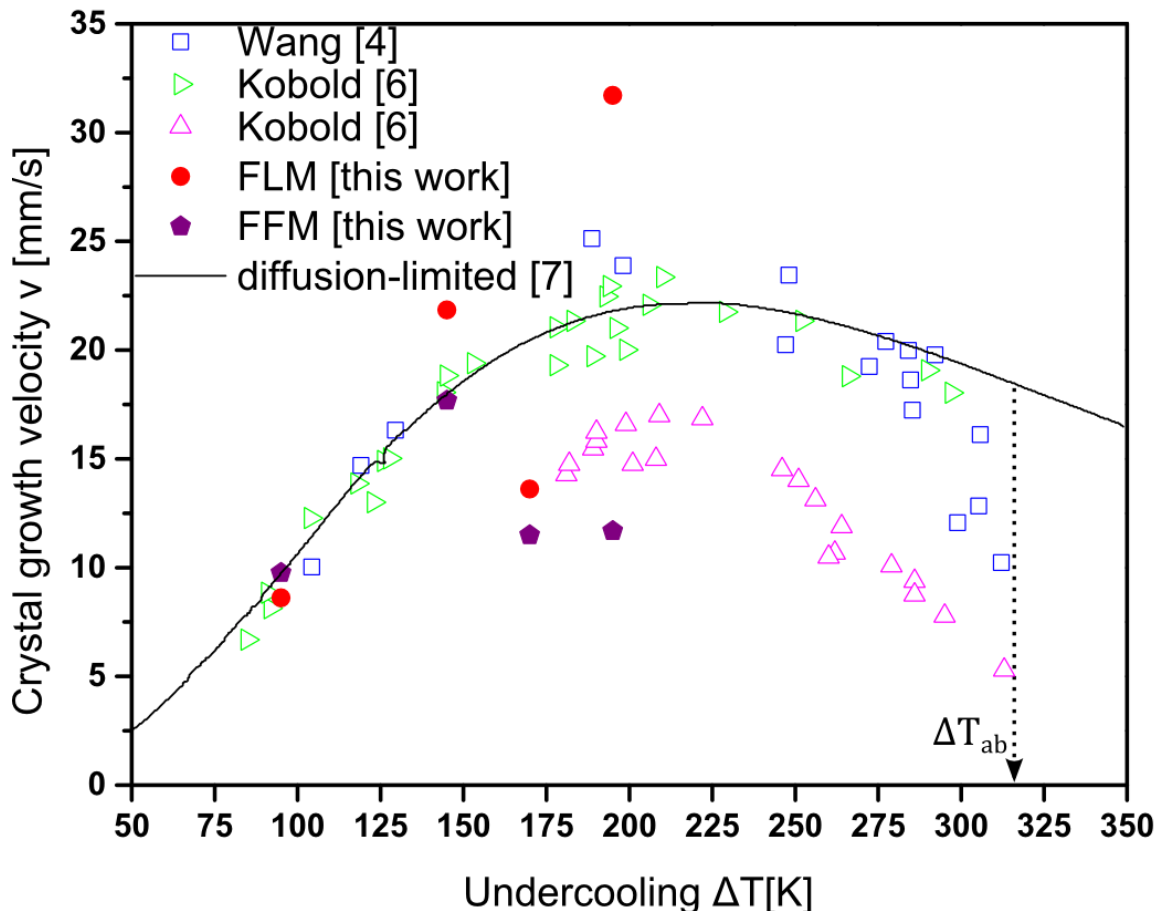


Figure 3. Solidification kinetics in $\text{Cu}_{50}\text{Zr}_{50}$. Experimental data for dendrite growth velocity were obtained by different authors (see insert). Theoretical model is given by Wang et al. [7] using a diffusion-limited approach. Results of the present work have been obtained using high-speed camera in an Electromagnetic Levitator under microgravity conditions during parabolic flights. They are shown for two different evaluation methods of recalescence fronts velocities: Frame by Frame Method (FFM) and First Frame-Last Frame Method (FLM). The critical undercooling ΔT_{ab} (or range of undercooling around ΔT_{ab}) shows the undercooling where an abrupt decrease of the solidification velocity in experimental data occurs – other than in the theoretical curve showing monotonic and gradual decrease of the velocity.

As is shown in Fig. 3, at undercoolings above the one with the velocity peak, the theoretical curve increasingly overestimates the experimental data of Wang et al. [4]. At the undercooling $\Delta T_{ab} \approx 320\text{K}$, experimentally measured velocities abruptly decrease. Note that such an abrupt transition has also been confirmed in other glass-forming Zr-Cu-Ni alloys with primary solidification of the CuZr-phase [11].

5. Discussion

As we have shown in the previous section, the solidification kinetics of the glass forming CuZr alloy exhibits several distinguished features that are not described theoretically so far (see Fig. 3). These features are related to the clearly observable velocity peak, the second sequence of experimental data for lower velocity values (in comparison with the main and complete data for the upper velocity sequence), and the abrupt decrease of the velocity at very high undercoolings. In the present section, we only discuss them in the light of experimental and modeling data for the dynamic viscosity. Theoretical predictions on the basis of these data will be presented and discussed in forthcoming publications.

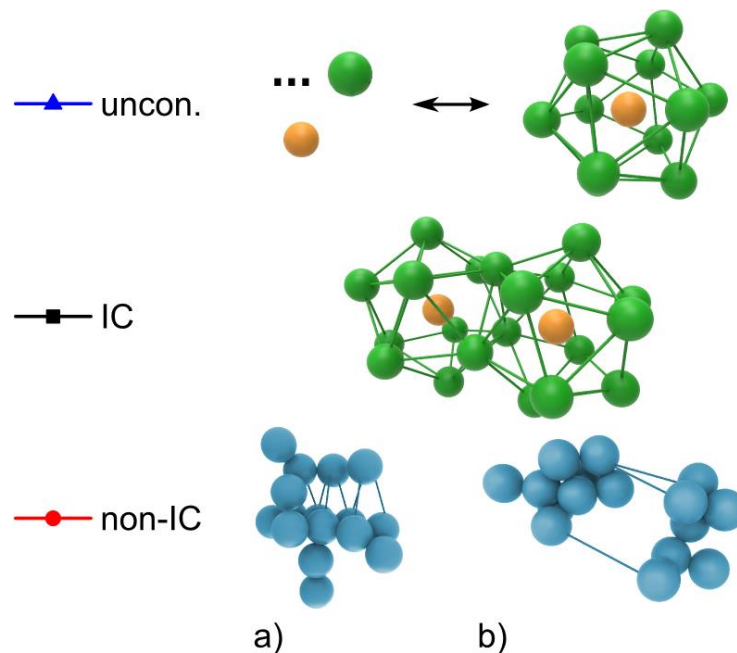


Figure 4. Cluster structures in $\text{Cu}_{50}\text{Zr}_{50}$ melt obtained *via* molecular dynamics simulations and Voronoi tessellation analysis [12]. Top: "uncon." structures are represented by unconnected single Zr or Cu atoms (left) and by single clusters (right). Middle: IC structures are represented by interpenetrating clusters – five atoms are shared between two shells. Bottom: non-IC structures are represented by vertex-, edge- or face-sharing clusters with a) pinning and/or b) bridging connection. Note that icosahedral clusters are unique structural elements of every non-IC-structure which thus is represented by a net of interpenetrating clusters.

5.1. Viscosity behaviour

Figure 4 depicts atomistic structures obtained in molecular dynamics simulations [12]. They are represented by isolated atoms or clusters that one can consider as a completely disordered structure of the overheated to slightly undercooled $\text{Cu}_{50}\text{Zr}_{50}$ melt (top of Fig. 4). In the deeply undercooled $\text{Cu}_{50}\text{Zr}_{50}$ melts, in Ref. [12] a double-connected or multiple-connected cluster structure was found (middle and bottom row of Fig. 4). These connected structures already show features of the ordering process in the undercooled melt, with a gradual transition from a "strong" liquid phase to "fragile" liquid phase (so-called fragility transition). Dominant structures in the liquid states are of controversy. If a coordination number of 12 is set, then icosahedral clusters as Kelton et al. via molecular simulations [12] suggest can be presumed present. This however was not confirmed experimentally by Holland-Moritz et al. [13] who find the nearest-neighbor coordination number Z_{NN} to be 13,8 and therefore the corresponding structure cannot be of icosahedras primarily but an aggregate of different other polyhedral structures. For the present consideration, it is not important which type of cluster structure exists in the undercooled melt. The present analysis takes into account clusterization and net of cluster construction as a process leading to glass formation. Critical points for beginning, developing and freezing of net of clusters are important for our understanding of the viscosity behaviour and kinetics of solidification.

Figure 5 (top) shows the structural ordering in CuZr melts as a content in percent amongst clusters. These results were obtained using molecular dynamic simulations in different states, particularly the overheated state $T > T_1$ state, at the melting temperature $T = T_1$, in the supercooled state $T < T_1$ and in a glassy state, $T \leq T_g$ by Kelton et al. [12]. These authors found three distinguishable structures, which are a) unconnected structures constantly building and collapsing from Cu and Zr atoms, b) interpenetrating clusters, where five atoms coincide on two shells (IC) and c) vertex-, edge-, or face-sharing polyhedrals with a pinning and/or bridging connections between Cu atoms (non-IC).

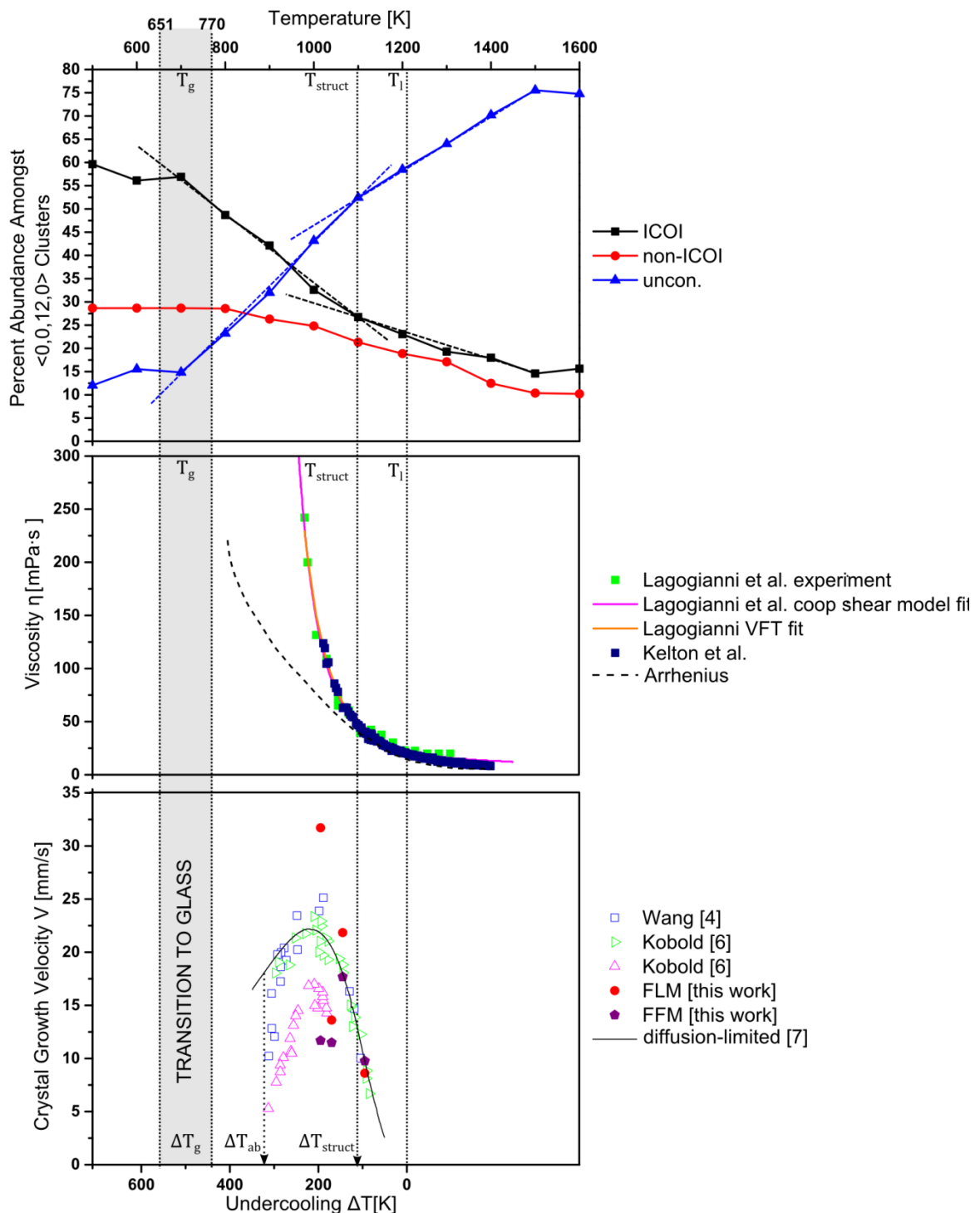


Figure 5. Top: structural ordering in the $\text{Cu}_{50}\text{Zr}_{50}$ melt obtained via molecular dynamics simulations and Voronoi tessellation analysis [12]. Uncon.- IC, non-IC, pinning and/or bridging connected structures are shown in Fig. 4. Middle: viscosity data by Kelton and Laggagio, fitting curves calculated using the cooperative shear model and Vogel-Fulcher-Tamman equation (VFT) and sketch of Arrhenius behavior (dashed line). Bottom: dendrite growth velocity as a function of undercooling. Groups of points (obtained in EML under different conditions) clearly show upper and lower branches in solidification kinetics.

Overheated and slightly undercooled liquid, i.e. in the temperature range $T_{\text{struct}} < T < T_1$, is characterized by a gradual decrease of the number of unconnected clusters and single atoms. The number of interconnected clusters, IC, gradually increases in this region. At $T = T_{\text{struct}}$, the intensity of cluster formation drastically changes, exhibiting a breakpoint from which IC forms more readily. Interconnected clusters (IC) rapidly form a cluster net, which results in a structural transition from a strong liquid (atomically disordered liquid) to a fragile liquid (atomically ordered liquid). This fragility transition ends at the glass temperature T_g at which a transition from the liquid state to the amorphous state occurs.

These structural changes strongly influence the viscosity as a function of temperature. Indeed, Kelton et al. [14] and Lagogianni et al. [15] studied the viscosity behavior in superheated and supercooled CuZr melts. In a modeled fit to their data sets [14,14], Lagogianni et al. applied the viscosity data most accurately in the whole temperature range of the viscosity change. With a cooperative shear model for the glass transition they derive a double-exponential dependence of viscosity from temperature (non-Arrhenius behavior) according to

$$\frac{\eta(T)}{\eta_0} = \exp \left\{ \frac{V_C C_G}{kT} \exp \left[(2 + \lambda) \alpha_T T_g \left(1 - \frac{T}{T_g} \right) \right] \right\} \quad (3)$$

with η_0 being a normalisation constant set by the high temperature limit of η , V_C being the characteristic atomic volume, C_G the shear modulus value at the glass transition temperature T_g , λ a variable expressing all salient features of interatomic interactions and containing the effect of repulsion steepness, and α_T the anharmonicity. A plot of Eq. (3) is shown in Fig. 5(middle), fitting the data sets of the groups of both Lagogianni and Kelton.

Taking into account Fig. 5(top) and evaluating the changes in behavior for unconnected / connected clusters / IC, the temperature for the beginning of the structural changes can be estimated as $T_{\text{struct}} \approx 1100$ K. At $T = T_{\text{struct}}$, a change from Arrhenius behavior to super-Arrhenius behavior of viscosity may occur as suggested by Eq. (4) and as drawn in Fig. 5 (middle). The change in behavior can be displayed more clearly when plotting $\ln \frac{\eta}{\eta_0}$ over $1000/T$ as an Arrhenius plot; the temperature below which a deviation from Arrhenius behavior occurs can then clearly be seen¹. Such structural changes may drastically influence the solidification kinetics of the undercooled Cu₅₀Zr₅₀ alloy melts.

The transition to the glassy state in Fig. 5 is shown as a shaded region of temperatures ranging from 651 K to 770 K. The existence of a temperature range for the transition is not surprising, because the temperature T_g characterizes a freezing of the non-equilibrium state which may vary due to different solidification conditions into the non-ergodic glassy state. Therefore, we have just marked the temperature interval in which various authors found the amorphous phase in solidification of Cu₅₀Zr₅₀ melts [4,15,17,18,19].

5.2. Solidification kinetics

The described changes in the liquid cluster structure and the viscosity behavior of liquids drastically influence the kinetics of dendritic growth in the undercooled Cu₅₀Zr₅₀ melts. This follows straightforwardly from the solidification growth velocity V described in Ref. [20]

$$V = \beta_k \left[1 - \exp \left(- \frac{\Delta G}{RT} \right) \right], \quad (4)$$

¹ Kelton et al. [16] have estimated this significant temperature as $T_{\text{coop}} \approx 1283$ K, 183,72 K higher than T_{struct} and indicating that the change in the cluster behavior proceeds at higher temperatures.

where the Gibbs free energy change upon solidification, ΔG , has been estimated by Thompson and Spaepen [21] as

$$\Delta G(T) = \frac{\Delta H_m \Delta T}{T_1} \left(\frac{2T}{T_1 + T} \right) \quad (5)$$

with the undercooling $\Delta T = T_1 - T$. As stated by Jäntschi [21], the kinetic growth coefficient β_k is inversely proportional to the dynamic viscosity η , i.e. $\beta_k \propto \eta^{-1}$. For the diffusion-limited process of atom attachment to the solid through the solid-liquid interface, Orava and Greer suggest the following expression [20]:

$$\beta_k = \frac{kT}{3\pi a^2 \eta}, \quad (6)$$

where a is an effective atom diameter. As a result, cluster evaluation and viscous behavior give a qualitative answer on the non-linear relationship velocity vs. undercooling for the dendrite growth kinetics in undercooled melts of $\text{Cu}_{50}\text{Zr}_{50}$.

Figure 5 (bottom) further demonstrates dendrite growth velocities as a function of undercooling in consistence with the transitive temperature intervals of the cluster changes and viscosity behavior. The undercooling ΔT_{struct} is marked at which the deviation from the linear behavior $V = \beta_k \Delta T$ begins. Comparing with the marked temperature $T = T_{\text{struct}}$, one should state that the beginning of the sharp increase of connected clusters, Fig. 5 (top), and the beginning of super-Arrhenius law in viscosity, Fig. 5 (middle), are directly related to the beginning of non-linearity in the solidification velocity by the full equation (4).

At undercoolings below the one that correlates with the velocity maximum (see short explanations for Fig. 3), Fig. 5 (bottom) also exhibits the second critical undercooling ΔT_{ab} which shows an abrupt decrease of the solidification velocity (also marked in the diagram “velocity-undercooling” of Fig. 3). This abrupt drop of the growth velocity at the largest undercooling has also been observed in $\text{Zr}_{50}\text{Cu}_{30}\text{Ni}_{20}$ [11] and in $\text{Ni}_{40}\text{Al}_{60}$ [23]. Considering that this drop occurs at a temperature close to the glass temperature ($\approx 60 \text{ K} + T_g$), it can be attributed to the fact that in this temperature region the single atom movement changes to a cooperative movement of atoms according to the mode coupling theory [24]. This is consistent with the fact that also the temperature dependence of the self-diffusion coefficient shows deviations from an Arrhenius-like behavior in this temperature range [25]. To describe this steep decrease at ΔT_{ab} , the model of diffusion-limited growth [7] should be expanded.

6. Conclusions

In the present work, a systematic review of experimental data on solidification of $\text{Cu}_{50}\text{Zr}_{50}$ alloy melts is presented. The data are collected from results of droplet solidification in different levitators (EML and ESL) used on Ground-based research and during parabolic flights in the TEMPUS facility. Structural changes of clusters in the melt drastically change dynamic viscosity and dendrite growth velocity in the undercooled melt. Theoretical models of solidification and amorphization can be developed using the present analysis of clustering and structural changes in undercooled glass forming alloy melts. In this perspective, the model of the diffusion-limited growth [7] should be expanded concerning two issues: first, the model should incorporate metastable phase formation, taking into account phase selection; second, the model should include the specific processes at T_{struct} and T_{ab} to describe the abrupt decrease of the growth velocity at high undercoolings.

7. References

- [1] Herlach D M, Galenko P K and Holland-Moritz D 2007 *Metastable Solids From Undercooled Melts* (Elsevier: Amsterdam)
- [2] Binder S, Galenko P K and Herlach D M 2014 The effect of fluid flow on the solidification of Ni_2B from the undercooled melt *Journal of Applied Physics* **115** 053511-1-11
- [3] Turnbull D 1950 Formation of crystal nuclei in liquid metals *J. Appl. Phys.* **21** 1022–1028
- [4] Wang Q et al. 2011 Diffusion-controlled crystal growth in deeply undercooled melt on

- approaching the glass transition *Physical Review B* **83** 014202-1-014202-5
- [5] Blodgett M E, Egami T, Nussinov Z. and Kelton K F 2015 Proposal for universality in the viscosity of metallic liquids *Sci. Rep.* **5** 13837
- [6] Kobold R 2016 Crystal growth in undercooled melts of glass forming Zr-based alloys *PhD-Dissertation (Ruhr-University: Bochum)*
- [7] Wang H, Herlach D M, Liu R P 2014 Dendrite growth in Cu₅₀Zr₅₀ glass-forming melts, thermodynamics vs. kinetics *EPL (Europhysics Letters)* **105** 36001
- [8] Herlach D M 1991 Containerless Undercooling and Solidification of Pure Metals *Annual Review of Materials Science* **21** 23-44
- [9] Herlach D M, Willnecker R and Lohöfer G 1989 *German Patent* DE 3639973
- [10] Volkmann T 2012 *In Solidification of Containerless Undercooled Melts* (Wiley-VCH)
- [11] Galenko P K, Hanke R, Paul P, Kobold R, Koch S and Rettenmayr M 2016 Unpublished results from parabolic flights
- [12] Soklaski R, Nussinov Z, Markow Z, Kelton K F and Yang L 2013 Connectivity of the Icosahedral Network and a Dramatically Growing Static Length Scale in Cu-Zr Binary Metallic Glasses *Phys. Rev. B* **87** 184203
- [13] Holland-Moritz D, Yang F, Kordel T, Klein S, Kargl F, Gegner J, Hansen T, Bednarcik J, Kaban I, Shuleshova O, Mattern N and Meyer A 2012 Does an icosahedral short-range order prevail in glass-forming Zr-Cu melts? *EPL* **100** 56002
- [14] Mauro N A, Blodgett M, Johnson M L, Vogt A J and Kelton K F 2014 A structural signature of liquid fragility *Nature Communications* **5** 4616
- [15] Lagogianni A E, Krausser J, Evenson Z, Samwer K and Zaccone A 2016 Unifying interatomic potential, $g(r)$, elasticity, viscosity, and fragility of metallic glasses: analytical model, simulations, and experiments *Journal of Statistical Mechanics: Theory and Experiment* 084001
- [16] Blodgett M, Egami T, Nussinov Z and Kelton K F 2014 Unexpected Universality in the Viscosity of Metallic Liquids [arXiv:1407.7558](https://arxiv.org/abs/1407.7558)
- [17] Lee D, Zhao B, Perim E, Zhang H, Gong P, Gao Y, Liu Y, Toher C, Curtarolo S, Schroers J and Vlassak J J 2016 Crystallization behavior upon heating and cooling in Cu₅₀Zr₅₀ metallic glass thin films *Acta Materialia* **121** 68-77
- [18] Wang W H, Lewandowski J J and Greer A L 2005 Understanding the glass-forming ability of Cu₅₀Zr₅₀ alloys in terms of a metastable eutectic *J. Mater. Res.* **20** 2307–2313
- [19] Yu P, Bai H Y and Wang W H 2006 Superior glass-forming ability of CuZr alloys from minor additions *Journal of Materials Research* **21** 1674–1679
- [20] Orava J, Hewak D W and Greer A L 2015 Fragile-to-Strong Crossover in Supercooled Liquid Ag-In-Sb-Te Studied by Ultrafast Calorimetry *Advanced Functional Materials* **25** 4851–4858
- [21] Thompson C V, Spaepen F 1979 On the approximation of the free energy change on crystallization *Acta Metallurgica* **27** 1855-1859
- [22] Jäntschi O 1956 *Zur Theorie der linearen Kristallisationsgeschwindigkeit unterkühlter Schmelzen - first part of dissertation* (Humboldt-University: Berlin)
- [23] Lengsdorf R, Holland-Moritz D and Herlach D M 2009 Anomalous dendrite growth in undercooled melts of Al-Ni alloys in relation to results obtained in reduced gravity *Scripta Materialia* **62** 365–367
- [24] Das S P 2004 Mode-coupling theory and the glass transition in supercooled liquids *Rev. Mod. Phys.* **76** 785-845
- [25] Yang F, Holland-Moritz D, Gegner J, Heintzmann P, Kargl F, Yuan C C, Simeoni G G and Meyer A 2014 Atomic dynamics in binary Zr-Cu liquids *EPL* **107** 46001

Acknowledgements

P.K.G. R.H., Ph.P., S.K., M.R., D.M.H. and W.D. are grateful to the German Space Agency for funding contract number 50WM1541, Project MULTIPHAS. P.K.G. also acknowledges the support from the RSF (project no. 16-11-10095). E.V.H. acknowledges financial support from the Russian Space Agency and TSNIIMash under project “Kinetika” (contract No. 0521).